McStas and Scatter Logger driven calculations of prompt gamma shielding for neutron guides

Rodion Kolevatov

Department for Neutron Materials Characterization, Institute for Energy Technology, NO-2027, Kjeller, Norway
E-mail: rodion.kolevatov@ife.no

Abstract. McStas ScatterLogger component bundle was adapted for evaluating a contribution to dose rate around neutron guides arising from prompt gamma radiation accompanying neutron capture in the supermirror guide coating upon specular reflection. Thickness of typical shielding materials needed to reduce this contribution to the desired level can be now evaluated directly from running a ray-tracing simulation of the instrument in McStas. An overview of the corresponding modifications to the existing McStas components and description of the newly written supplementary ones is given together with examples and use instructions.

Keywords: McStas, neutron guides, shielding

1. Introduction

At contemporary high flux neutron sources the neutrons are transported at rather large distances from the source to the sample position, typically several tens of meters. Effective transport of neutrons over such distances is achieved by using neutron guides with "supermirror" coatings of the walls. A "supermirror" consists of multiple bilayers of materials with strong neutron optical contrast and varying thickness. It allows for an m-fold increase in the angle of total reflection compared to that of nickel. Upon reflection, a neutron typically penetrates to a certain depth in the coating where bilayer thicknesses satisfy the Bragg reflection condition. When considering the low incidence angle of a reflected neutron, this would imply a path length of up to a few millimeters in the materials of the coating. Consequently, a certain fraction of neutrons are captured in the coating materials at each reflection giving rise to high energy prompt photon emission. Its amount along the guide varies depending on transported flux, spectrum and divergence together with m-value and reflectivity of the guide coating. The correct account for this contribution is critical for the guide shielding design.

An idea to use ray-tracing software for accounting for losses of neutrons during transport in order to address production of prompt photons along the guide was put forward some time ago. A special code for use in McStas ray-tracing package [1–3], Scatter Logger bundle, was developed capable of tracking and processing changes in the neutron states upon each reflection in the neutron optics [4]. The original Scatter Logger bundle allowed access to the characteristics of the non-reflected neutrons, such as loss position, incidence angle, energy etc. However, it didn't implement a full picture of reflection from a supermirror. It was not possible to distinguish between neutrons captured in the materials of the guide coating with the release of high energy prompt gamma radiation and those transmitted into the guide substrate, typically a borosilicate glass, giving rise mostly to a comparatively low energy gamma radiation from capture by boron. Existing implementations of supermirror in PHITS and MCNP transport Monte-Carlo codes suffer from similar deficiencies, although work on improving the situation for MCNP is currently ongoing [5].

Results of a recent calculation of neutron absorption in supermirror coatings [6,7], together with consideration of guide substrate waviness effects on shielding [8], allow to single out the two contributions upon data recorded by the Logger. This opens an opportunity for rigorous calculations of the neutron capture in particular materials and, given the prompt gamma spectra, evaluation of the dose rates and shielding requirements directly from running a ray-tracing model of the neutron instrument. Description of the corresponding modifications to the components of the Scatter Logger bundle which allow to do so, constitute the subject of the present paper.

In Section 2, an overview of results of the studies [6,7] and [8] is given while Section 3 contains details of their implementation in McStas components. In Section 4, we illustrate the use for the particular case of shielding of the ESS BIFROST [9] instrument. Section 5 concludes the article.

2. Neutron absorption in the guide coating

2.1. Reflection with $q > q_c^{Ni}$

In [6,7] capture probabilities in the multilayer coatings per incident neutron were calculated for multilayer compositions used in commercial production of supermirrors ($m = 1.6 \ldots 6$) at SwissNeutronics. When momentum transfer at reflection exceeds a critical value for total reflection from nickel, $q_c^{Ni} = 0.0218$ Å^{-1}, the reflection occurs at bilayers following the outermost nickel layer of the coating. In this case, the probabilities of absorption in coating materials per incident neutron, f_a, are conveniently described as functions of a ratio of neutron momentum transfer at reflection $q_\perp$ to the critical value q_c^{Ni}, $\mu = q_\perp/q_c^{Ni}$. The functions have a parametric dependence on the coating m-value with two distinct regimes:

- Momentum transfer below supermirror cutoff $1 < \mu < m$

$$f_a^{Ni}(\mu) = 0.005 + 0.005(\mu - 1) \tag{1}$$

$$f_a^{Ti}(\mu) = 0.00027 + 0.00027(\mu - 1) \tag{2}$$

- Momentum transfer beyond supermirror cutoff, $\mu > m$

$$f_a^{Ni}(\mu) = 0.0025(m + 0.1)^2/\mu \tag{3}$$

$$f_a^{Ti}(\mu) = 0.00225(m - 0.9)(m + 0.1)/\mu \tag{4}$$

2.2. Low angle reflection, effect of waviness

At reflection with low momentum transfer neutrons typically don't penetrate beyond the outermost nickel layer of the coating and the parametric dependencies given by (1) and (2) don't hold [7]. For momentum transfer at reflection below critical value q_c^{Ni} and a perfectly even layer surface, the reflection loss is typically below 0.01%. This is in contrast with an empirical value of $0.5 \div 1\%$ ($99 \div 99.5\%$ low angle reflection probability) commonly accepted for describing neutron transport in the guides. Attributing the low-angle reflectivity loss fully to neutron interaction in the coating would thus overestimate neutron capture and would lead to way too conservative estimates and unnecessary overshielding of the guide.

The main reason for the low-angle reflectivity loss is however waviness of the reflecting surface which effectively increases beam divergence.[1] When an angle of grazing incidence is considered with respect to the local normal to the surface, a certain fraction of neutrons falls beyond the coating cutoff and are not transported further. Typical values for the waviness[2] of $\lesssim 10^{-4}$ rad [10] translate to approximately $0.5 \cdot 10^{-4}$ rad variation of the grazing angle

---

[1] Author is especially thankful to Marton Marko and Mads Bertelsen for explaining this point.

[2] The waviness is defined as r.m.s. angle between the two vectors normal to the surface averaged over the surface area.

at the reflection point. At a wavelength $\lambda = 5$ Å this corresponds to a $\delta k_\perp \approx 6.3 \cdot 10^{-5}$ Å^{-1} variation of the normal momentum component which constitutes around 0.6% of the critical momentum for nickel, $k_c^{\text{Ni}} = 0.5 \cdot q_c^{\text{Ni}} = 0.0109$ Å^{-1}. With a uniform distribution of the grazing incidence angle from zero to cutoff ($k_\perp = 0 \ldots k_c^{\text{Ni}}$), a fraction of transported neutrons around $\sim \delta k_\perp / k_c^{\text{Ni}}$ will appear beyond the cutoff and will not be reflected. The number is consistent with 0.5–1% loss of the reflectivity at low angles which is commonly accepted for the neutron optics calculations.

Probability of capture per non-reflected neutron at low angles for an $m = 1$ single layer coating hence can be evaluated as capture probability per incident neutron in the first reflection minimum beyond the critical momentum transfer. A calculation of this quantity was performed in [8] and the following conservative estimate was derived:

$$\bar{f}_a^{\text{Ni}}\big(q < q_c^{Ni}\big) = \frac{\sigma_a(\lambda)}{\sigma_a(\lambda) + \sigma_d(\lambda)}\big[1 - e^{-6\text{Im}(k_{\text{min}}^{\text{Ni}})d}\big] \tag{5}$$

where $k_{\text{min}}^{\text{Ni}}$ stands for normal component of a neutron wave vector in the Ni layer of thickness d when the coating is hit at reflection minimum.[3] The reflection minimum is defined from a destructive interference condition for the reflected wave:

$$d \cdot \text{Re}k_{\text{min}}^{\text{Ni}} = \pi. \tag{6}$$

$\sigma_a(\lambda)$ and $\sigma_d(\lambda)$ denote wavelength dependent cross sections for neutron capture and diffuse scattering respectively.

Correspondingly, for a multilayer coating with $m > 1$ the probability per non-reflected neutron at low angles can be evaluated as capture probability per incident neutron at the reflection threshold (Eqs (1) and (2) with $\mu = m$).

3. Extension of McStas Scatter Logger functionality

3.1. Recording neutron capture

A description of a neutron instrument within McStas ray-tracing Monte-Carlo package is written in a meta-language. It is composed of predefined or user-supplied *components* placed according to the real setup of the instrument under consideration in a text file. The original Scatter Logger bundle enables logging and processing details of neutron interactions within parts of the instrument contained between `Scatter_Logger` and `Scatter_Logger_Stop` components. A subsequent `Scatter_Log_Iterator` component iterates through the recorded states and propagates pseudo-neutrons with non-reflected weight and pre-collision momentum starting from the interaction point. Characteristics of non-reflected neutrons can then be explored and recorded by various McStas components of type `Monitor`.

Extending functionality of the Scatter Logger in order to address neutron capture in the coating materials includes several key steps. First, neutron capture probability at reflection depends on the m-value of the coating. Correspondingly, a number of McStas components which are commonly used in construction of the guide systems were customized in order to allow logging of the m-value at reflection point by assigning a value to a global variable at each neutron interaction. The corresponding modifications were made to the following key components: `Guide`, `Guide_curved` (be used instead of `Bender` component, was modified to have the same syntax for the input parameters), `Elliptic_guide_gravity` and `Guide_chanelled`.

Second, the original `Scatter_Logger` component was updated in order to include the m-value at the reflection point to the saved state (in addition to neutron states before and after the reflection as it was originally).

---

[3]Wave vector of a neutron in an absorbing medium is complex-valued since a potential entering Schrödinger equation for the neutron wave function acquires an imaginary part which accounts for absorption and diffuse scattering [11].

A possibility to have more than one `Scatter_Logger` component in the instrument, that is record neutron states in different parts of the instrument independently was also implemented. To avoid confusion with original components, an updated component was named `Shielding_Logger`.

Finally, in addition to an original iterator component pair which processes the buffer of saved states and returns weight of the non-reflected neutrons, two new iterator components were written, `Shielding_Log_Iterator_Ni` and `Shielding_Log_Iterator_Ti`, which implement parameterizations Eqs (1)–(5) and propagate neutron weights corresponding to the capture in the correspondent materials of the coating. The same buffer of saved states is processed three times by the three iterators which are placed in the McStas instrument file one after another. This also required some minor modifications to the original `Scatter_Log_Iterator` component (when iterator is the last one in the line one must specify that explicitly to clean the memory) which after modification was renamed to `Shielding_log_iterator_total`. Neutron capture rate in particular materials along the guide can be addressed by the standard `Monitor_ND` McStas component which would write the output to a text file.

The syntax of the logger and iterator components is similar to the syntax of the original constituents of the Scatter Logger bundle and the relevant examples of use may be found in the McStas repository.

3.2. Dose rate and shielding parameters evaluation from a McStas simulation

In general, there are several contributions to the dose rate around the guide (e.g. high energy neutrons, slow neutron scattered from beam windows or escaping through the gaps between guide segments and others). However, in many cases, for example outside the line of sight to the neutron source, the prompt gammas coming from neutron capture in the guide coating dominate the dose rate. Capture rates of neutrons in the coating material and in the substrate along the guide calculated in McStas can be used to define a corresponding source term for a transport Monte-Carlo simulation. Equivalently, they can be used for a direct numerical evaluation of the prompt gamma contribution to the dose rate and assessment of guide shielding requirements.

For a mono-energetic photon source, the dose rate beyond lateral shielding H can be obtained as a product of uncollided source photon fluence rate, energy dependent fluence to effective dose conversion factor $K(E)$ and a buildup factor $B(E, x)$ [12,13]. The buildup factor accounts for a contribution to the effective dose from scattered radiation arriving at the detection point and depends on both the energy of primary photons and their optical path length. For a particular case of guide shielding, once the radiation energy spectrum and intensity along the neutron guide $I(E, z)$ is known, the photon fluence rate is obtained via integrating $I(E, z)$ along the guide with account of attenuation due to distance and traversed material thickness. The expression for the effective dose thus takes on the form (for notations see Fig. 1):

$$H(R, z) = \frac{1}{4\pi} \int dz\, dE\, K(E) I(E, z) B\big(E, \mu d(z)\big) \frac{1}{R^2 + z^2} e^{-\mu(E)d(z)} \tag{7}$$

where $d(z) = \frac{(R - R_0)\sqrt{R^2 + z^2}}{R}$.

The energy dependent linear attenuation coefficient μ, dose buildup $B(E, \mu d)$ and flux to dose conversion coefficient $K(E)$ are table values available from the literature on radiation protection [13–16].
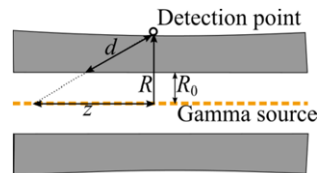

Fig. 1. Geometry for the dose rate evaluation outside lateral guide shielding at the surface.

For the two newly written components in McStas performing dose rate calculations and evaluating shielding needs, it is assumed that the non-reflected neutrons which are not captured in the coating are captured in the borosilicate guide substrate. Although neutron capture in the borosilicate glass occurs presumably by boron atoms, a small fraction of neutrons transmitted to the substrate are captured by other elements, in particular silicon, with release of photons with energy of several MeV. The McStas components thus implement equation (7), interpolation of table values for $\mu(E)$, $B(E, x)$, $K(E)$ for some typical shielding materials and, finally, spectra of prompt gamma radiation per neutron capture in nickel, titanium and borosilicate glass. The spectra are calculated using cross sections of (n, γ) reactions from a Prompt Gamma Activation Analysis datafile available at [17].

The `Dose_calculator` component calculates dose rate outside lateral shielding of a specified material with fixed thickness at its surface along the neutron guide. The `Shielding_calculator` component evaluates shielding thickness required to reach given dose rate at a shielding surface outside as one moves along the guide. A user can choose from a few common shielding materials (lead, iron, light concrete) and the presence or absence of an inner iron shielding layer of a specified thickness. The components simply read the output of the `Monitor_nD` monitors placed within the three iterators as described in Section 3.1 (the names of output files for the monitors which must have identical binning have to be specified) and perform the requested calculations. The components may be run from a separate McStas file which doesn't contain the description of an instrument. In this case, a user has to provide a path to the files which contain pre-calculated capture in Ni, Ti and overall loss along the guide.

The components were benchmarked to a measurement of a gamma dose rate along the PSI instruments (mostly $m = 2$ guides) shielded with 120 mm steel and a good correspondence between the calculation and measurement was obtained [8].

4. Usecase example: ESS BIFROST

As an illustration of the potential application a result of dose rate calculation along a part of the guide system of BIFROST instrument is presented. BIFROST will be constructed among the first eight instruments at the European Spallation Source. Up to the distance of 28 meters from moderator the guide system passes through a heavily shielded bunker, where it is curved to avoid the line of sight to the neutron source just before the 3.5 m thick heavy concrete wall of the bunker. The curving has a large effect for reducing contribution from fast neutrons to the overall level of ionizing radiation around the guide beyond the bunker wall [18], so the prompt gamma radiation from neutron capture in the coating will dominate the dose rate. The instrument will have a shutter blocking the cold neutron beam at 48 meters to allow maintenance of the chopper placed at 78 meters and operations in the instrument cave at 162 meters from the moderator.

The source of the prompt gamma radiation along the guide was obtained by running a McStas model of the BIFROST instrument developed by Jonas O. Birk and Rasmus Toft-Petersen, with the actual configuration of the neutron optics including the m-value distribution.

A shielding configuration under examination consisted of 10 cm steel followed by 30 cm of heavy concrete for the first 2 meters after the bunker wall and 10 cm steel with 40 cm of regular concrete beyond this point. This configuration was chosen on the basis of an evaluation of thicknesses via `Shielding_calculator` so as to not exceed 1 μSv/hr at the shielding surface. A numerical calculation of the dose rate via `Dose_calculator` was performed along with a FLUKA [19,20] simulation of the same setup. FLUKA transport Monte-Carlo code allows for the writing of a custom source routine which would generate primaries according to the capture rates along the guide calculated in McStas and prompt gamma emission spectra. The agreement between the two results is quite good as seen in Fig. 2, although dose rate calculated according to (7) is slightly higher. This may be a result of using precalculated buildup factors for the infinite medium in the direct numerical evaluation.

In Fig. 3 a result of a FLUKA simulation for one of the use-cases of the BIFROST instrument is plotted. Here a neutron beam is dumped into a shutter composed of a B_4C followed by a lead plate. The plot is a sum of two contributions. The first one is prompt gamma radiation resulting from neutron capture along the guide as described above. The second one is the neutron beam dumped in the shutter. To evaluate the latter contribution a McStas
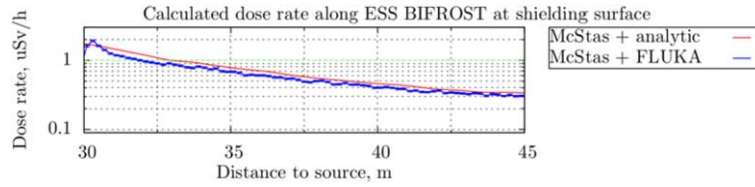
Fig. 2. Dose rate along ESS BIFROST guide shielding at the surface calculated according to (7) and using FLUKA.
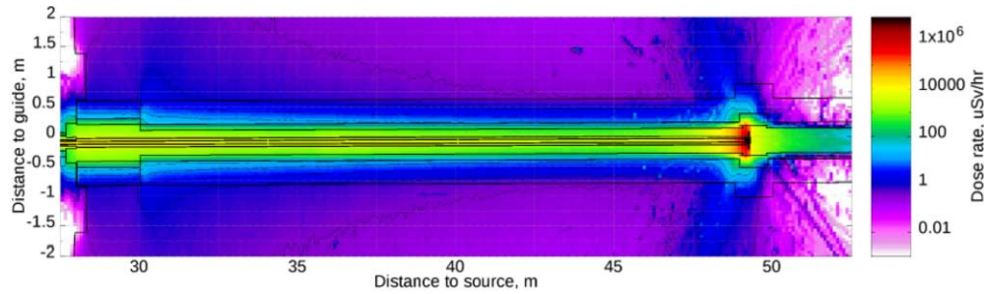

Fig. 3. Dose rate distribution in the shielding around BIFROST guide, cut by horizontal plane at guide height.

simulation of the instrument was performed with recording neutron states crossing the guide section at 48 meters in a MCPL format file [21], a capability which is included in standard functionality of McStas. The pre-compiled C-language libraries which contain routines for reading MCPL files were then linked to a FLUKA executable at compilation together with writing another custom user-defined source routine. The routine generated primaries by reading neutron states from the MCPL output of a McStas simulation. The input file for the simulation containing the description of the guide and shielding geometry was prepared with the help of CombLayer [22,23].

5. Conclusions

The functionality of the McStas Scatter Logger bundle was extended in order to allow for a fast and reliable evaluation of one of the major contributions to dose rate around neutron guides arising from prompt gamma radiation accompanying capture of neutrons of the transported beam in the supermirror guide coating. Calculated capture rates in the coating materials can be used as a source term in a transport Monte-Carlo simulation of the guide shielding.

References

[1] K. Lefmann and K. Nielsen, McStas, a general software package for neutron ray-tracing simulations, *Neutron News* **10**(3) (1999), 20–23. doi:10.1080/10448639908233684.

[2] P. Willendrup, E. Farhi and K. Lefmann, McStas 1.7 – A new version of the flexible Monte Carlo neutron scattering package, *Physica B: Condensed Matter* **350**(1–3) (2004), E735–E737. doi:10.1016/j.physb.2004.03.193.

[3] P. Willendrup, E. Farhi, E. Knudsen, U. Filges and K. Lefmann, McStas: Past, present and future, *Journal of Neutron Research* **17**(1) (2014), 35–43. doi:10.3233/JNR-130004.

[4] E.B. Knudsen, E.B. Klinkby and P.K. Willendrup, McStas event logger: Definition and applications, *Nuclear Instruments and Methods in Physics Research Section A: Accelerators, Spectrometers, Detectors and Associated Equipment* **738** (2014), 20–24. doi:10.1016/j.nima.2013.11.071.

[5] M. Magan, Private communication.

[6] R. Kolevatov, C. Schanzer and P. Böni, Neutron absorption in supermirror coatings, *Journal of Neutron Research* **20**(4) (2018), 127–129. doi:10.3233/JNR-180088.

[7] R. Kolevatov, C. Schanzer and P. Böni, Neutron absorption in supermirror coatings: Effects on shielding, *Nuclear Instruments and Methods in Physics Research Section A: Accelerators, Spectrometers, Detectors and Associated Equipment* **922** (2019), 98–107. doi:10.1016/j.nima.2018.12.069.

[8] R. Kolevatov, Prompt gamma shielding of neutron guides from ray-tracing Monte-Carlo simulations, *Journal of Surface Invetigation: X-ray, Synchrotron and Neutron Techniques* (2020), in press.

[9] P. Freeman, J.O. Birk, M. Markó, M. Bertelsen, J. Larsen, N.B. Christensen, K. Lefmann, J. Jacobsen, C. Niedermayer, F. Juranyi et al., CAMEA ESS – The continuous angle multi-energy analysis indirect geometry spectrometer for the European Spallation, *EPJ Web of Conferences* **83** (2015), 03005.

[10] https://www.swissneutronics.ch/products/neutron-guides/.

[11] V.F. Sears, Fundamental aspects of neutron optics, *Physics Reports* **82**(1) (1982), 1–29. doi:10.1016/0370-1573(82)90151-X.

[12] J.K. Shultis and R.E. Faw, *Radiation Shielding*, 2nd edn, American Nuclear Society, La Grange Park, IL, 2000.

[13] V.P. Mashkovich and A.V. Kudryavtseva, *Ionizing Radiation Protection: A Handbook*, 4th edn, Energoatomizdat, Moscow, 1995, in Russian.

[14] J. Hubbel and S. Seltzer, Tables of X-ray mass attenuation coefficients and mass energy-absorption coefficients from 1 keV to 20 MeV for elements $Z = 1$ to 92 and 48 additional substances of dosimetric interest, 1989, 1990, 1996, 2005.

[15] I.C. on Radiological Protection, *Radiological Protection, ICRP Publication 74: Conversion Coefficients for Use in Radiological Protection Against External Radiation*, Vol. 23, Elsevier Health Sciences, 1996.

[16] N. Kucuk, Computation of gamma-ray exposure buildup factors up to 10 mfp using generalized feed-forward neural network, *Expert Systems with Applications* **37**(5) (2010), 3762–3767. doi:10.1016/j.eswa.2009.11.047.

[17] Prompt gamma activation analysis database files, https://www-nds.iaea.org/pgaa/databases.htm.

[18] R. Kolevatov, Simulating BIFROST instrument to 35 meters from the source, Technical Report, ESS-0511506, 2018.

[19] T. Böhlen, F. Cerutti, M. Chin, A. Fassò, A. Ferrari, P. Ortega, A. Mairani, P. Sala, G. Smirnov and V. Vlachoudis, The FLUKA code: Developments and challenges for high energy and medical applications, *Nuclear data sheets* **120** (2014), 211–214. doi:10.1016/j.nds.2014.07.049.

[20] A. Ferrari, P.R. Sala, A. Fasso and J. Ranft, FLUKA: A multi-particle transport code (Program version 2005), Technical Report, CERN-2005-10, INFN/TC_05/11, SLAC-R-773, 2005.

[21] T. Kittelmann, E. Klinkby, E.B. Knudsen, P. Willendrup, X.X. Cai and K. Kanaki, Monte Carlo particle lists, *Mcpl, Computer Physics Communications* **218** (2017), 17–42. doi:10.1016/j.cpc.2017.04.012.

[22] A. Milocco, G. Gorini, L. Zanini and S. Ansell, The CombLayer build of the MCNPX models for the design of the fast neutron ports in the European Spallation source, in: *SNA+ MC 2013 – Joint International Conference on Supercomputing in Nuclear Applications + Monte Carlo*, EDP Sciences, 2014, p. 05207.

[23] https://github.com/SAnsell/CombLayer.

[24] V. Vlachoudis et al., FLAIR: A powerful but user friendly graphical interface for FLUKA, in: *Proc. Int. Conf. on Mathematics, Computational Methods & Reactor Physics (M&C 2009)*, Vol. 1, Saratoga Springs, New York, 2009, p. 3.

[25] http://www.essworkshop.org/.